Chemistry–A European Journal
Research Article
doi.org/10.1002/chem.202303079
Chemistry Europe
European Chemical Societies Publishing
www.chemeurj.org

Hot Paper

# Oxidation-state sensitive light-induced dynamics of Ruthenium-4*H*-Imidazole complexes

Linda Zedler,[a] Stephan Kupfer,[b] Heiner Schmidt,[a, b] and Benjamin Dietzek-Ivanšić*[a, b, c]

Oxidized molecular states are key intermediates in photo-induced redox reactions, e.g., intermolecular charge transfer between photosensitizer and catalyst in photoredox catalysis. The stability and longevity of the oxidized photosensitizer is an important factor in optimizing the respective light-driven reaction pathways. In this work the oxidized states of ruthenium(II)-4*H*-imidazole dyes are studied. The ruthenium complexes constitute benchmark photosensitizers in solar energy interconversion processes with exceptional chemical stability, strong visible light absorption, and favourable redox properties. To rationalize the light-induced reaction in the oxidized ruthenium(III) systems, we combine UV-vis absorption, resonance Raman, and transient absorption spectroelectrochemistry (SEC) with time-dependent density functional theory (TDDFT) calculations. Three complexes are compared, which vary with respect to their coordination environment, i.e., combining an 4*H*-imidazole with either 2,2′-bipyridine (bpy) or 2,2′;6′2″-terpyridine (tpy) coligands, and chloride or isothiocyanate ligands. While all oxidized complexes have similar steady state absorption properties, their excited state kinetics differ significantly; the study thus opens the doorway to study the light-driven reactivity of oxidized molecular intermediates in intermolecular charge transfer cascades.

## Introduction

Molecular processes underlying artificial photosynthesis typically involve changes in the oxidation state of the photosensitizers or catalysts as part of photoinduced intermolecular electron transfer.[1] Upon light absorption electronically excited photosensitizers undergo either oxidative or reductive quenching as part of the reaction cascade ultimately leading to the function of the molecular artificial photosynthetic system (Scheme 1). To obtain a comprehensive understanding of the photophysical pathways and potentially optimizing the efficiency of molecular systems for solar energy conversion the photophysics of the oxidized (or reduced) intermediates has to be understood. Work in this context – in particular studying transition metal complexes, as benchmark molecular photosensitizers – has been devoted to developing pump-pump-probe spectroscopy,[2] *in operando* transient absorption[3] (TA) and *in situ* resonance Raman (rR) spectroscopy,[4] as well as IR-absorption,[5] resonance Raman,[6] emission and transient absorption spectroelectrochemistry (SEC).[7] In particular the latter approach enables the controlled production of intermediates in chemically inert solvents, i.e., in the absence of sacrificial donors, acceptors or substrates for catalytic conversion, followed by their spectroscopic characterization.

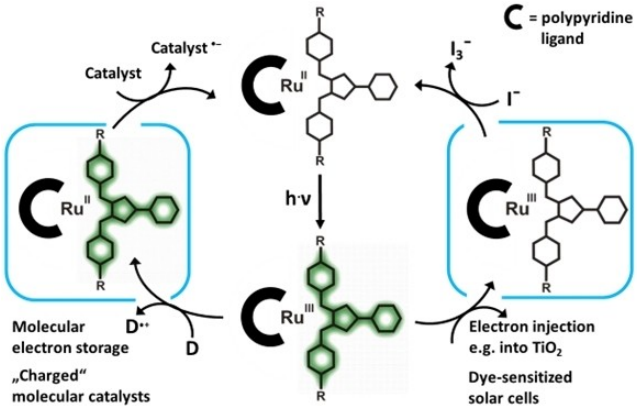


**Scheme 1.** In situ monitoring of spectroscopic changes accompanying electrochemical processes is of utmost importance for mechanistic understanding of the single and multiple electron-transfer processes occurring during light induced energy conversion, i.e., in photo-catalytic cycles (left) or in dye-sensitized solar cells (right). Both cycles involve the generation of short-lived reactive intermediates (reduced (left) or oxidized (right) dyes) the direct observation of which is only possible by spectro-electrochemical techniques.

Ruthenium(II)-polypyridyl dyes present benchmark photosensitizers and are widely used in solar energy conversion due

[a] L. Zedler, H. Schmidt, Prof. Dr. B. Dietzek-Ivanšić
Functional Interfaces
Leibniz Institute of Photonic Technology
Albert-Einstein-Straße 9, 07745 Jena, Germany
E-mail: benjamin.dietzek@uni-jena.de
benjamin.dietzek@leibniz-ipht.de
linda.zedler@leibniz-ipht.de

[b] Dr. S. Kupfer, H. Schmidt, Prof. Dr. B. Dietzek-Ivanšić
Institute of Physical Chemistry
Friedrich Schiller University Jena
Helmholtzweg 4, 07743 Jena, Germany

[c] Prof. Dr. B. Dietzek-Ivanšić
Jena Center for Soft Matter
Friedrich Schiller University Jena
Philosophenweg 7, 07743 Jena, Germany

Supporting information for this article is available on the WWW under https://doi.org/10.1002/chem.202303079

to their exceptional chemical stability, strong visible light absorption, and distinctive redox and catalytic properties.[8] This contribution focusses on the excited-state dynamics in a set of complexes featuring a 4*H*-imidazole ligand together with either 2,2′-bipyridine (bpy) or 2,2′;6′2″-terpyridine (tpy) ligands (Figure 1). The complexes have a broad and intense absorption in the visible spectrum, due to the presence of strong metal-to-ligand charge transfer ($^1$MLCT) and ligand centred ($^1$LC) transitions and are stable in several redox states. While the photophysics of the complexes in the parent Ru(II) oxidation state has been investigated,[9] comparably little is known about the light-induced processes in their oxidized form, i.e. when the central metal ion is present as Ru(III). This, however, represents the key intermediate if the photosensitizers are used in n-type dye-sensitized solar cells (DSSCs); light absorption by the dye is followed by rapid electron injection into the band gap of the semiconductor.[10] Subsequently, the oxidized dye persists as an intermediate on the surface of the semiconductor before it is re-reduced by a redox couple, e.g., iodine/iodide (Scheme 1).

Using rR-SEC, we have previously investigated the oxidized state of the (isothiocyanato-$\eta$3-4,4′,4″-tri-*tert*-butyl-2,2′:6′,2″-terpyridine-$\eta$2-2-(4-carboxyphenyl)-4,5-(*p*-tolylimino)-imidazolate-ruthenium(II) (**tpyRuImNCS-COOH**) (Figure 1B) on $TiO_2$ as model for a functional photoanode as well as the absorption and vibrational features of the oxidized dyes **tpyRuImNCS** and **tpyRuImNCS-COOH**.[7] While these studies let us conclude that the complexes present promising structures for multi-photo-electron donors in DSSCs we did not investigate the excited-state dynamics of this class of sensitizers in their oxidized state, i.e., the state representing the oxidized intermediate in any functional photoanode (Scheme 1).

The work presented here addresses this topic and combines UV-Vis-SEC and rR-SEC with TA-SEC to analyse the excited state dynamics and excited state lifetimes of three different Ru-4*H*-imidazolato dyes in solution. The experimental data is complemented by in depth theoretical calculations to address the ground and excited state properties of the redox intermediates in different protonation states. As the coordination sphere is key for the photophysics, we compare the excited state dynamics of **RuIm** complexes bis(4,4′-di-*tert*-butyl-2,2′-bipyridine-κ$^2$*N,N′*)[2-(4-carboxyphenyl)-4,5-bis(*p*-tolylimino-κ*N*)-imidazolato]-ruthenium(II) (**bpy$_2$RuImH-COOH**), isothiocyanato-$\eta$3-4,4′,4″-tri-*tert*-butyl-2,2′:6′,2″-terpyridine-$\eta$2-2-(4-carboxyphenyl)-4,5-(*p*-tolylimino)-imidazolate-ruthenium(II) (**tpyRuImNCS-COOH**) and chloro-$\eta$3-4,4′,4″-tri-*tert*-butyl-2,2′:6′,2″-terpyridine-$\eta$2-2-phenyl-4,5-(*p*-tolylimino)-imidazolate-ruthenium(II) (**tpyR-**

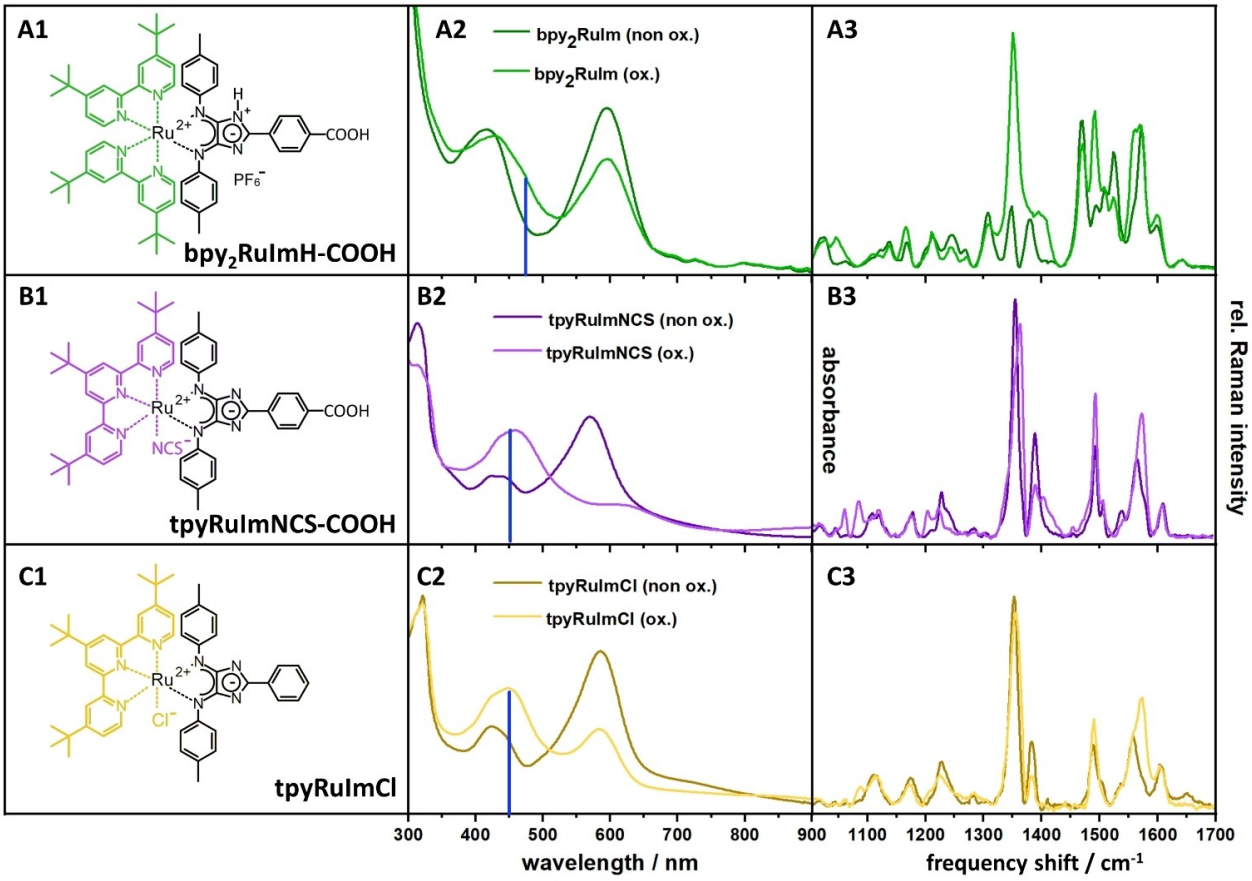


**Figure 1.** A1–C1: Molecular structure of the complexes under investigation. A2–C2: UV-vis spectra of non-oxidized and singly oxidized **bpy$_2$RuImH-COOH** (green), **tpyRuImNCS-COOH** (purple) and **tpyRuImCl** (yellow) recorded in acetonitrile containing 0.1 M $TBABF_4$ electrolyte (glassy carbon working, Pt-counter and Ag/AgCl-pseudo reference electrodes). Resonance Raman excitation wavelengths are displayed as vertical lines in the UV-vis spectra; 473 nm (A2) and 458 nm (B2, C2). A3–C3: RR-SEC spectra of the non-oxidized (dark) and oxidized (bright) complexes.

**uImCl**), carrying either bpy or tpy ligands (Figure 1). Two of the investigated complexes contain a carboxyl group at the phenyl moiety of the 4*H*-imidazole ligand, as a potential anchoring side to an n-type semiconductor.

## Results and Discussion

### UV-Vis- and rR-SEC

In the parent oxidation state, the strong visible absorption of **bpy$_2$RuImH-COOH** stems from MLCT and LC transitions localized mainly on the 4*H*-imidazole ligand (Figure 1A2, ocp). In full agreement with earlier studies on structurally related systems, TDDFT simulations (B3LYP[11]/6-31G(d)[12]/MWB-28,[13] implicit solvent effects were taken into account by a polarizable continuum model[14] for acetonitrile; see supporting information for details) reveal that two strongly dipole-allowed $^1$MLCT$_{Im}$ transitions (into $S_3$ and $S_6$; Tables S3 and S4) contribute dominantly to the red absorption feature of **bpy$_2$RuImH-COOH**: The absorption at ~400 nm stems from intra-ligand charge transfer (ILCT) transition of the 4*H*-imidazol ligand (into $S_7$) and from one MLCT$_{bpy}$ (into $S_{10}$). Upon a potential deprotonation at the imidazole (**bpy$_2$RuIm-COOH**, Tables S1 and S2), the respective MLCT$_{im}$ states are shifted by approximately 0.2 eV to higher excitation energies. Upon $Ru^{II}\rightarrow Ru^{III}$ oxidation (see spin density of the doublet ground state, $D_0$) the MLCT band decreases (Figure 1A2, ox), while a new band appears at ~475 nm for the singly oxidized doublet species. The latter is attributed to two ILCT contributions localized on the 4*H*-imidazole ligand, i.e., associated with $D_{11}$ and $D_{15}$ predicted at 548 and 482 nm, respectively. Furthermore, dipole-allowed $^2$MLCT$_{Im}$ ($D_{24}$ at 437 nm) and ligand-to-ligand charge transfer ($^2$LLCT; $D_{27}$ at 416 nm) excitations from the bpy-ligand to the 4*H*-imidazole are modelled by TDDFT. Interestingly, the quantum chemical simulations reveal not only an energetically high-lying ligand-to-metal charge transfer ($^2$LMCT, $D_{37}$ at 390 nm) but also two low-lying and weakly dipole-allowed $^2$LMCT transitions, i.e., into $D_3$ and $D_4$ at 1107 and 840 nm. Such $^2$LMCT transitions lead to the initial $d^6$-low-spin redox state of the Ru, while the electron hole is shifted either to the electron rich tolyl moieties of the 4*H*-imidazole ligand ($D_3$ and $D_4$) or to the electron deficient bpy sphere ($D_{37}$). The structurally similar **tpyRuImNCS-COOH** and **tpyRuImCl** have been investigated previously by absorption and rR spectroscopy.[7,9a] Briefly, the MLCT absorption of **tpyRuImNCS-COOH** at 567 nm involves accepting orbitals on both the Im ($S_6$ at 452 nm; Tables S9 and S10) and the tpy ($S_7$ and $S_8$ at 497 and 490 nm) ligands. The strong absorption at 400–450 nm is due to an MLCT$_{tpy}$ to the terpyridine ligand ($S_9$ at 467 nm) as well as to mixed ILCT and MLCT$_{Im}$ transitions involving the 4*H*-imidazole ($S_{10}$ at 452 nm). Upon Ru(II)→Ru(III) oxidation (see $D_0$ spin density in Table S10) the MLCT absorption at 567 nm is reduced significantly, while the absorption at 450 nm increases due to an increase of the $^2$ILCT absorption ($D_{14}$, $D_{23}$ and $D_{26}$ at 510, 437 and 423 nm). Additionally, a broad and low intense absorption band evolves beyond 700 nm, which TDDFT associates with the weakly dipole-allowed excitations into the $D_3$ and $D_6$ LMCT states at 1044 and 684 nm, respectively. Further details concerning the TDDFT results can be found in the Supporting Information.

To further corroborate the interpretation of the electronic states contributing to the absorption properties and to identify oxidation-related structural changes in the chromophores rR-SEC was employed upon excitation at 473 nm (**bpy$_2$RuImH-COOH**) and 458 nm (**tpyRuImNCS** and **tpyRuImCl**), i.e., close to the maximum of the new absorption band. In the rR spectrum of the one-electron-oxidized **bpy$_2$RuImH** new intense bands appear at 1350, 1491 and 1560 $cm^{-1}$. Similar oxidation-induced features are observed for **tpyRuImNCS** and **tpyRuImCl**, e.g., the hypsochromic shift of the band at 1354 $cm^{-1}$, the reduction in intensity of the band at 1388 $cm^{-1}$ and the increase of the bands at 1492 and 1572 $cm^{-1}$ localized on the 4*H*-imidazole ligand.[7] Only the shoulder at 1330 $cm^{-1}$ can be attributed to the terpyridine ligand. Hence, upon oxidation of **bpy$_2$RuImH**, **tpyRuImNCS** and **tpyRuImCl**, mainly IL transitions at the 4*H*-imidazole ligand are excited at 473 nm and 458 nm, respectively while the contribution of MLCT transitions diminishes.

### Excited-state dynamics

To investigate the photoinduced dynamics not only in the Ru(II) but also in the Ru(III) complexes, we employed femtosecond TA-SEC (Figures 2 and 3) upon excitation at 403 and 467 nm ($75\pm15$ fs pulse duration and 0.64 $\mu J/cm^{-2}$ average pulse energy). The experimental data is amended by results from quantum chemical simulations. As summarized in Figure 2B, excitation of the parent **bpy$_2$Ru(II)ImH-COOH** at 403 nm, i.e., in resonance with the $^1$ILCT and $^1$MLCT$_{bpy}$ transition, yields transient absorption features reminiscent of those observed for related Ru-4*H*-Im complexes:[7,15] An excited-state absorption (ESA) between 450 and 550 nm is due to ligand-centred (LC) transitions in the formally reduced 4*H*-imidazole ligand. The ESA at around 700 nm stems from ligand-to-metal charge transfer transitions. The accompanying ground state bleach (GSB) at 600 nm agrees well with the UV-vis absorption spectrum of the oxidized complex (Figure 2A) indicating that strong ESA transitions are absent in this spectral range. The kinetics reflect the formation of a ligand-centred ESA at 485 nm (stemming from ligand-centred transitions of the formally reduced 4*H*-Im ligand) within 1 ps after excitation, which is followed by a decay of the entire differential absorption signal back to zero on a 200 ps timescale (Figure S1 A). In contrast to the ESA band at 485 nm, the evolution of which can be resolved in the TA-SEC experiments, the ESA signal at 700 nm (due to LMCT transitions) appears instantaneously upon excitation and decays also on a 200 ps timescale. Following previous studies, the light-induced processes at short delay times are assigned to $^1$MLCT→$^3$MLCT-ISC.[10] The relaxation to the ground state is quantitatively accounted for by a 135-ps time constant (Figure S1 B, DAS). To shed further light onto the light-induced processes in **bpy$_2$Ru(II)ImH-COOH**, we performed DFT and TDDFT simulations. In agreement with the experimental observations as well as with the literature,[10] the lowest triplet state is

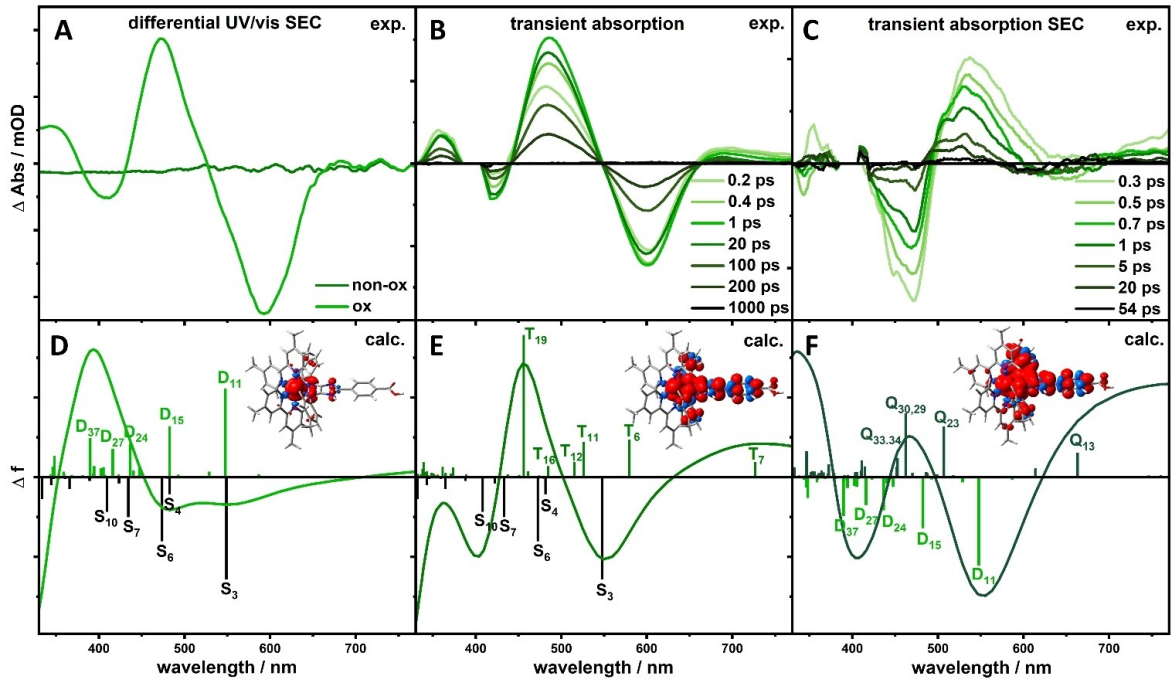


**Figure 2.** Differential UV-vis spectroelectrochemical changes during the first oxidation of **bpy$_2$RuImH-COOH** (A). Transient absorption spectra at selected delay times of the neutral (B), and oxidized **bpy$_2$RuImH-COOH** (C) pumped at 403 nm. The ground state bleach of the photoexcited oxidized complex at 470 nm essentially corresponds to the UV-vis-SEC spectrum (mirrored on the horizontal axis). Simulated differential UV-vis-SEC spectrum of **bpy$_2$RuImH-COOH** (D) as obtained by the spin and dipole-allowed excitations of the non-oxidized singlet species (negative signal) and singly oxidized doublet species (positive signal). Simulated TA (E) and TA-SEC (F) spectra as obtained based on TDDFT simulations of the non-oxidized singlet and the non-oxidized triplet species as well as by the singly oxidized doublet and the singly oxidized quartet species, respectively. Prominent electronic transitions are indicated. Electronic ground state characters are indicated for $D_0$ ($d_{Ru}$, D), $T_1$ ($^3$MLCT$_{Im}$, E) and $Q_1$ ($^4$ILCT, F).

found to be of $^3$MLCT$_{Im}$ nature (spin density inset in Figure 2E and $T_1$ in Table S4). Simulations relate the ESA at ~700 nm to an excitation into the $T_7$ $^3$LMCT state (725 nm), while the prominent ESA feature between 450 and 550 nm is mainly associated with a $^3$ILCT transition ($T_{19}$ at 455 nm). Additional $^3$ILCT contributions in this spectral range arise from $T_8$ and $T_{11}$ (at 579 and 525 nm, respectively) as well as from the $^3$LMCT transitions into $T_{12}$ and $T_{16}$ (at 514 and 483 nm).

Of particular interest is $T_{16}$, as this state is associated with a $^3$MC species (i.e., $d^5_{eg}$, $d^1_{t2g}$), the population of which are well known, excited-state relaxation pathways in (pseudo−)octahedral d$^6$ transition metal complexes.[16]

Time-resolved measurements of the oxidized **bpy$_2$Ru(III)ImH-COOH** complex were recorded in a custom-made spectroelectrochemical cell upon oxidation of the complex at 0.85 V *vs.* Ag/AgCl pseudo reference in ACN/0.1 M $TBABF_4$ solution in a chronoamperometric fashion.[17] Pump pulses centred at 403 nm populate a mixture of ILCT and LLCT excited states. However, it should be noted that at this wavelength also the ILCT transition of non-oxidized **bpy$_2$Ru(II)ImH-COOH** is excited, if the electrochemical conversion is not complete (Figure 1A2). Thus, the TA spectra of the oxidized **bpy$_2$Ru(III)ImH-COOH** (Figure 2C) are extracted by calculating a scaling factor and subtracting the contribution of the non-oxidized **bpy$_2$Ru(II)ImH-COOH** from the experimentally obtained TA spectra (see Supporting Information for more details).

Figure 2C presents the obtained TA data of **bpy$_2$Ru(III)ImH-COOH**, which prompts the following observations: (i) the ground state bleach of the photoexcited oxidized complex at 470 nm reflects the spectral shape of the corresponding UV-vis-SEC spectrum. This underlines the validity of the numerical procedure to extract the transient absorption data of the oxidized species and leads to the conclusion that in the spectral range of ground state absorption no significant excited state absorption is observed. (ii) Between 500 and 770 nm a strong ESA of the oxidized complex is observed, which TDDFT ascribes to dominant contributions of ILCT transitions admixed by transitions of LMCT and MC character. Notably, the accuracy of the performed TDDFT simulations to assess the excited-state absorption of the quartet species is likely inferior with respect to the evaluation of the Franck-Condon photophysics of the previously studied non-oxidized species. These transitions involve the states $Q_{13}$, $Q_{23}$ and $Q_{29}$ at 663, 507 and 462 nm, respectively (see Supporting Information for more information). Upon increasing the delay time from zero to 20 ps, the ESA band decreases in intensity while undergoing a blue shift from 540 to 525 nm. (iii) In addition to the ESA peaking between 540 and 525 nm, an addition ESA band is observed at 750 nm. This band decays in less than 1 ps and hence significantly faster than the ESA at ca. 530 nm (Figure S1). This short lifetime suggests that ISC between the initially photoexcited doublet states to quartet states take place. TDDFT calculations confirm

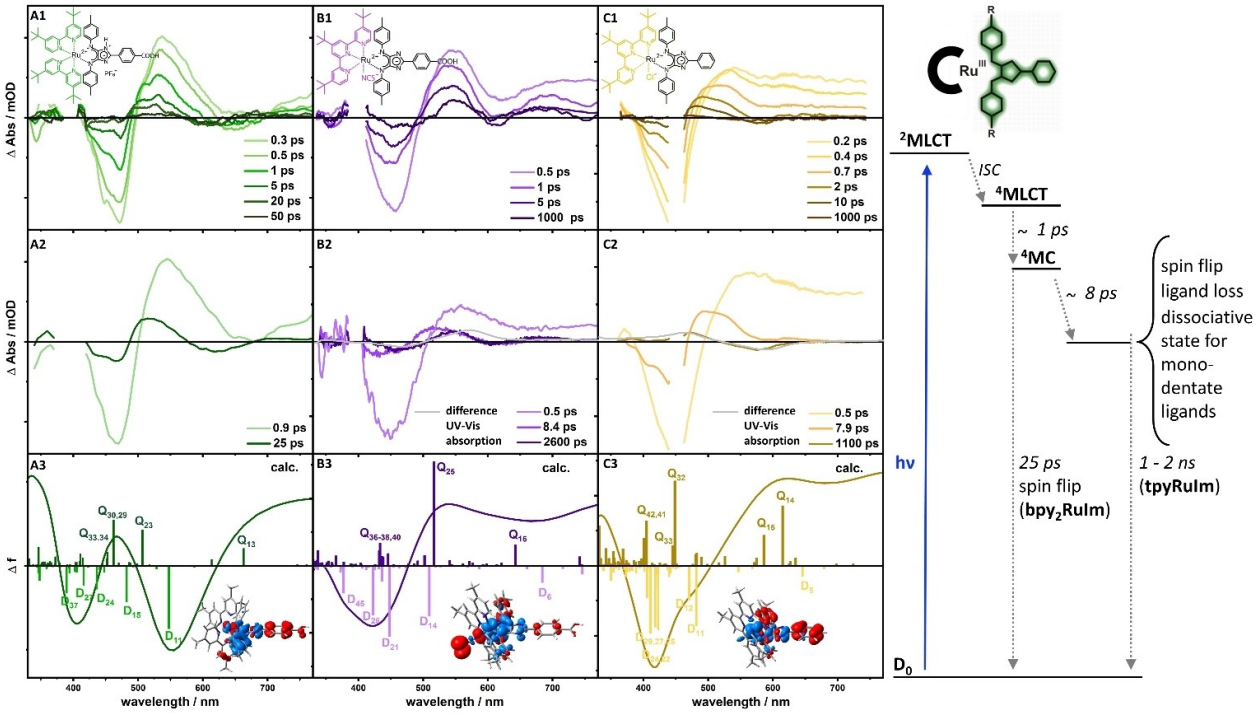


**Figure 3.** Transient absorption data including transient absorption spectra at selected delay times (A1–C1) and spectral changes associated with each kinetic process (DAS) (A2-C2) for singly-oxidized **bpy$_2$RuImH-COOH** (A), **tpyRuImNCS-COOH** (B) and **tpyRuImCl** (C), pumped at 403 nm (**bpy$_2$RuImH-COOH** and **tpyRuImNCS-COOH**) and 467 nm (**tpyRuImCl**). For comparison difference UV-Vis absorption spectra of oxidized complexes **tpyRuImNCS-COOH** and **tpyRuImCl** are plotted in the DAS panels (grey lines in B2 and C2). Right: Simplified energy level diagram of oxidized **bpy$_2$RuImH-COOH**, **tpyRuImNCS-COOH** and **tpyRuImCl**. Simulated TA-UV-vis-SEC spectra as obtained by the spin and dipole-allowed quartet-quartet (positive signal) and doublet-doublet transitions (negative signal) (A3–C3). Prominent electronic transitions are indicated.

that the quartet ground state ($Q_1$) with its spin density depicted in Figure 2F and Table S4 is accessible upon ISC and excited-state relaxation from the initially photoexcited doublet states. The $Q_1$ state is found to be of $^4$ILCT character, and the three unpaired electrons are localized in one $d_{eg}$ orbital of the Ru(III), as well as in one $\pi_{im}$ and one $\pi^*_{im}$ orbital. (iv) We analyse the transient absorption data of **bpy$_2$Ru(III)ImH-COOH** by global fitting, which yields the decay associated spectra (DAS) depicted in Figures 3A2 and S1. The spectral changes reflected in the DAS are associated with two characteristic time-constants, $\tau_1 = 0.9$ ps and $\tau_2 = 25$ ps. In line with the arguments presented before, we ascribe the process associated with $\tau_1$ to transitioning electron density from the $\pi^*$ orbital of the 4*H*-imidazole ligand into an empty d-orbital of Ru(III), i.e., population of the metal-centred $Q_4$ state via a $^4$LMCT processes. The subsequent ground state recovery occurs upon another spin flip with the characteristic time constant $\tau_2$.

In addition to **bpy$_2$Ru(III)ImH-COOH**, also the structurally related complexes **tpyRu(III)ImNCS-COOH** and **tpyRu(III)ImCl** were investigated concerning their photophysics in the oxidized forms. The complexes differ in the nature of the polypyridine ligand sphere and we investigate the influence of structural ligand modification, i.e., introduction of a carboxyl group in the para position of the phenyl group directly binding to the 4*H*-imidazole ring.[7,10]

Figures 3 and S2 depict the results from TA-SEC of the singly oxidized complexes upon excitation at 403 nm, i.e., in resonance with the $^2$ILCT transition centred on the 4*H*-imidazole. The data reveal an instantaneous GSB between 400 and 500 nm, i.e., in the spectral range of maximum steady-state absorption of the oxidized complexes (see Figure 1). The respective bleach is accompanied by an ESA from 500 to around 600 nm for all three compounds. For **tpyRu(III)ImNCS-COOH** and **tpyRu(III)ImCl** the ESA extends to longer probe wavelength than captured in the experiment. The long-wavelength ESA signal at 760 nm is less pronounced for **bpy$_2$Ru(III)ImH-COOH** compared to **tpyRu(III)ImNCS-COOH** and **tpyRu(III)ImCl**. Nonetheless, the decay of the respective long-wavelength ESA occurs on a similar timescale for all the complexes and is associated with a fast decay component, $\tau_1$, in the order of less than 1 ps (Figure 3A1–C1, S2).

When comparing the transient kinetics of the oxidized complexes, it is noticeable that the excited states are consistently significantly shorter-lived than their respective Ru(II) counterparts (Figure S2). Furthermore, it is obvious from the kinetics that the excited state of the oxidized bipyridine containing compound deactivates more rapidly than the oxidized complexes containing terpyridine ligands (Figure S2). The corresponding time constants to quantitatively compare the kinetic processes were obtained by global fitting of the TA-SEC data (Figure 3A2–C2). The fastest component, associated with $\tau_1$, are spectrally similar for all complexes and associated with ISC and rapid population of $^4$MC states. The second DAS of 25 ps corresponds to a spinflip and re-population of the ground

state in case of **bpy$_2$Ru(III)ImH-COOH** *via* a non-radiative LMCT (Figure 3, energy level diagram). We ascribe the rate difference observed for the decay of the $^4$MC state, i.e., $\tau_2 = 25$ ps for **bpy$_2$Ru(III)ImH-COOH**, while $\tau_2 = 8$ ps for **tpyRu(III)ImNCS-COOH** and **tpyRu(III)ImCl**, to the fact, that the bpy chelat ligands are not dissociating, but structurally rearranging during the decay of the $^4$MC state. In **tpyRu(III)ImNCS-COOH** and **tpyRu(III)ImCl** the $^4$MC state is associated with a weakening of the monodentate coordinative bond and hence the decay of the $^4$MC occurs upon ligand labilization on the 10-ps time scale.

The two complexes **tpyRu(III)ImNCS-COOH** and **tpyRu(III)ImCl** feature an additional long-lived component in the respective transient absorption data, which is absent in **bpy$_2$Ru(III)ImH-COOH** (Figure 3A2—3, C2). We ascribe the presence of this third, long-lived component to those complexes, in which the monodentate ligands $Cl^-$ and $NCS^-$ have been destabilized or dissociated. The longest component spectrum is very similar to the spectrum of the complex fragment, i.e., the complex without or with a prolonged bond between Ru and $NCS^-$ and $Cl^-$ (Figure 3B2 and C2, comparison of long-lived component with difference UV-Vis spectra of the oxidized complexes with monodentate ligands, grey line). Population of this long-lived species is likely facilitated both by the destabilization of the coordinative bond by metal oxidation and the photoinduced population of a $^4$MC state.

In **tpyRu(III)ImNCS-COOH** the weakening of the Ru-NCS bond originates mainly from a reduced π-back bonding. In the singly oxidized doublet species, this π-back bonding is already weakened due to the oxidation of the metal centre or rather due to the electron hole in the respective $\pi_{Ru-NCS}$ orbital. However, this bond is even further weakened upon ISC and subsequent relaxation via $^4$LMCT processes. These LMCT processes lead to the population of $^4$MC states (e.g., $Q_4$, $Q_7$, $Q_8$, $Q_9$ and $Q_{10}$) where an electron from the 4*H*-imidazole ligand is excited into an $\pi^*_{Ru-NCS}$ orbital, which may eventually lead to the dissolution of the $NCS^-$ ligand. The situation for **tpyRu(III)ImCl** is slightly different, as the chloride ligand is a pure σ-donor and does not feature additional π-acceptor properties. Thus, the respective coordinative bond is more prone to dissociation. In consequence, this effect is larger for the lighter $Cl^-$ ligand and the dissociation is faster. Therefore, the characteristic lifetime associated with the 3$^{rd}$ DAS ($\tau_3 = 1100$ ps) is smaller for **tpyRu(III)ImCl** than for **tpyRu(III)ImNCS-COOH**. Thus, the significantly enhanced lifetimes in the tpy containing Ru(III) complexes is associated with light-induced dissociation of the monodentate ligand.

## Conclusions

To understand the excited state dynamics of molecular intermediates in intermolecular electron transfer cascades, which are key to artificial photosynthesis, we present a combined approach of steady-state and time-resolved spectroelectrochemistry with TDDFT calculations. Here, we focus on the excited-state relaxation properties of oxidized ruthenium-4*H*-imidazole photosensitizers. The results obtained from resonance Raman and transient absorption spectro-electrochemistry highlight the general trend that the excited states of the oxidized **bpy$_2$Ru(III)ImH-COOH**, **tpyRu(III)ImCl** and **tpyRu(III)ImNCS-COOH** decay rapidly via a metal-centred ($^4$MC) state. However, the ground-state recovery of the oxidized tpy containing complexes is significantly, i.e., by two orders of magnitude, slower due to labilization of the monodentate co-ligand. Therefore, multidentate ligand coordination as in **bpy$_2$Ru(III)ImH-COOH** avoids ligand labilization or dissociation and therefore ensures a greater long-term stability by significantly reducing the lifetime of the damageable excited state. The lowest energy excited state transition is observed in the near IR region for all three oxidized complexes. The deactivation pathway in these complexes after ILCT excitation involves population of the $^4$MC state followed by ISC back to the ground state.

## Supporting Information

The Supporting information contains details regarding the TDDFT results such as excitation wavelengths and energy, oscillator strengths and excited-state characters.[11,12–14,17,18] Furthermore, the numerical procedure to extract the transient absorption signatures of the oxidized complexes from the experimentally recorded transient absorption spectra is described.

## *Acknowledgements*

This research was financially supported by the German Science Foundation (CATALIGHT CRC/Transregio 234 (project A1, A4 and C1) and SPP 2102 "Light-controlled reactivity of metal complexes" (project no. 494988281 and 404382951)). The calculations were performed at the Universitätsrechenzentrum of the Friedrich-Schiller University of Jena. Open Access funding enabled and organized by Projekt DEAL.

## *Conflict of Interests*

The authors declare no conflict of interest.

## *Data Availability Statement*

The data that support the findings of this study are available from the corresponding author upon reasonable request.

**Keywords:** photocatalysis · quantum chemistry · Ruthenium(II)-4*H*-imidazole · spectro-electrochemistry · transient absorption

[1] a) D. Gust, T. A. Moore, A. L. Moore, *Acc. Chem. Res.* **2001**, *34*, 40–48; b) D. Gust, T. A. Moore, A. L. Moore, *Acc. Chem. Res.* **2009**, *42*, 1890–1898.

[2] a) M.-H. Ha-Thi, V.-T. Pham, T. Pino, V. Maslova, A. Quaranta, C. Lefumeux, W. Leibl, A. Aukauloo, *Photochem. Photobiol. Sci.* **2018**, *17*, 903–909; b) M. Kuss-Petermann, O. S. Wenger, *Helv. Chim. Acta* **2017**, *100*, e1600283.
[3] a) M. Forster, D. W. F. Cheung, A. M. Gardner, A. J. Cowan, *J. Chem. Phys.* **2020**, *153*, 150901; b) I. Grigioni, L. Ganzer, F. V. A. Camargo, B. Bozzini, G. Cerullo, E. Selli, *ACS Energy Lett.* **2019**, *4*, 2213–2219.
[4] a) L. Zedler, P. Wintergerst, A. K. Mengele, C. Müller, C. Li, B. Dietzek-Ivanšić, S. Rau, *Nat. Commun.* **2022**, *13*, 2538; b) D. Chen, X. Xiong, B. Zhao, M. A. Mahmoud, M. A. El-Sayed, M. Liu, *Adv. Sci.* **2016**, *3*, 1500433.
[5] D. C. Jagesar, F. Hartl, W. J. Buma, A. M. Brouwer, *Chem. Eur. J.* **2008**, *14*, 1935–1946.
[6] a) L. Zedler, J. Guthmuller, I. Rabelo de Moraes, S. Kupfer, S. Krieck, M. Schmitt, J. Popp, S. Rau, B. Dietzek, *Chem. Commun.* **2014**, *50*, 5227–5229; b) L. Zedler, S. Krieck, S. Kupfer, B. Dietzek, *Molecules* **2019**, *24*, 245; c) L. Zedler, J. Guthmuller, I. Rabelo de Moraes, S. Krieck, M. Schmitt, J. Popp, B. Dietzek, *J. Phys. Chem. C* **2013**, *117*, 6669–6677; d) J. Schindler, S. Kupfer, L. Zedler, M. Wächtler, S. Gräfe, A. A. Ryan, M. O. Senge, B. Dietzek, *ChemPhysChem* **2016**, *17*, 3480–3493.
[7] Y. Zhang, S. Kupfer, L. Zedler, J. Schindler, T. Bocklitz, J. Guthmuller, S. Rau, B. Dietzek, *Phys. Chem. Chem. Phys.* **2015**, *17*, 29637–29646.
[8] a) S. Campagna, F. Puntoriero, F. Nastasi, G. Bergamini, V. Balzani, *Photochemistry and Photophysics of Coordination Compounds I*, *280*, 117–214; b) V. Balzani, A. Juris, *Coord. Chem. Rev.* **2001**, *211*, 97–115; c) H.-W. Tseng, R. Zong, J. T. Muckerman, R. Thummel, *Inorg. Chem.* **2008**, *47*, 11763–11773; d) C. Busche, P. Comba, A. Mayboroda, H. Wadepohl, *Euro J of Inorganic Chem* **2010**, *2010*, 1295–1302; e) A. Islam, H. Sugihara, H. Arakawa, *J. Photochem. Photobiol. A* **2003**, *158*, 131–138; f) A. Hagfeldt, G. Boschloo, L. Sun, L. Kloo, H. Pettersson, *Chem. Rev.* **2010**, *110*, 6595–6663; g) V. Balzani, A. Juris, M. Venturi, S. Campagna, S. Serroni, *Chem. Rev.* **1996**, *96*, 759–834; h) L. Zedler, S. Kupfer, I. R. de Moraes, M. Wächtler, R. Beckert, M. Schmitt, J. Popp, S. Rau, B. Dietzek, *Chemistry* **2014**, *20*, 3793–3799.
[9] a) S. Kupfer, J. Guthmuller, M. Wächtler, S. Losse, S. Rau, B. Dietzek, J. Popp, L. González, *Phys. Chem. Chem. Phys.* **2011**, *13*, 15580–15588; b) M. Wächtler, S. Kupfer, J. Guthmuller, J. Popp, L. González, B. Dietzek, *J. Phys. Chem. C* **2011**, *115*, 24004–24012.
[10] J. Schindler, S. Kupfer, M. Wächtler, J. Guthmuller, S. Rau, B. Dietzek, *ChemPhysChem* **2015**, *16*, 1061–1070.
[11] a) A. D. Becke, *J. Chem. Phys.* **1993**, *98*, 5648–5652; b) A. D. Becke, *Physical review. A, General physics* **1988**, *38*, 3098–3100; c) C. Lee, W. Yang, R. G. Parr, *Phys. Rev. B* **1988**, *37*, 785–789.
[12] P. C. Hariharan, J. A. Pople, *Theor. Chim. Acta* **1973**, *28*, 213–222.
[13] D. Andrae, U. Huermann, M. Dolg, H. Stoll, H. Preu, *Theor. Chim. Acta* **1990**, *77*, 123–141.
[14] J. Tomasi, B. Mennucci, R. Cammi, *Chem. Rev.* **2005**, *105*, 2999–3093.
[15] M. Wächtler, M. Maiuri, D. Brida, J. Popp, S. Rau, G. Cerullo, B. Dietzek, *ChemPhysChem* **2013**, *14*, 2973–2983.
[16] a) N. Sinha, O. S. Wenger, *J. Am. Chem. Soc.* **2023**, *145*, 4903–4920; b) K. S. Kjær, K. Kunnus, T.s C. B. Harlang, T. B. van Driel, K. Ledbetter, R. W. Hartsock, M. E. Reinhard, S. Koroidov, L. Li, M. G. Laursen, E. Biasin, F. B. Hansen, P. Vester, M. Christensen, K. Haldrup, M. M. Nielsen, P. Chabera, Y. Liu, H. Tatsuno, C. Timm, J. Uhlig, V. Sundström, Z.n Németh, D. Sárosiné Szemes, É. Bajnóczi, G. Vankó, R. Alonso-Mori, J. M. Glownia, S. Nelson, M. Sikorski, D. Sokaras, H. T. Lemke, S. E. Canton, K. Wärnmark, P. Persson, A. A. Cordones, K. J. Gaffney, *Phys. Chem. Chem. Phys.* **2018**, *20*, 4238–4249.
[17] a) S. Bold, L. Zedler, Y. Zhang, J. Massin, V. Artero, M. Chavarot-Kerlidou, B. Dietzek, *Chem. Commun.* **2018**, *54*, 10594–10597; b) L. Zedler, A. K. Mengele, K. M. Ziems, Y. Zhang, M. Wächtler, S. Gräfe, T. Pascher, S. Rau, S. Kupfer, B. Dietzek, *Angew. Chem. Int. Ed.* **2019**, *58*, 13140–13148.
[18] a) R. Siebert, D. Akimov, M. Schmitt, A. Winter, U. S. Schubert, B. Dietzek, J. Popp, *ChemPhysChem* **2009**, *10*, 910–919; b) C. Müller, T. Pascher, A. Eriksson, P. Chabera, J. Uhlig, *J. Phys. Chem. A* **2022**, *126*, 4087–4099; c) M. J. Frisch, G. W. Trucks, H. B. Schlegel, G. E. Scuseria, M. A. Robb, J. R. Cheeseman, G. Scalmani, V. Barone, G. A. Petersson, H. Nakatsuji, X. Li, M. Caricato, A. V. Marenich, J. Bloino, B. G. Janesko, R. Gomperts, B. Mennucci, H. P. Hratchian, J. V. Ortiz, A. F. Izmaylov, J. L. Sonnenberg, Williams, F. Ding, F. Lipparini, F. Egidi, J. Goings, B. Peng, A. Petrone, T. Henderson, D. Ranasinghe, V. G. Zakrzewski, J. Gao, N. Rega, G. Zheng, W. Liang, M. Hada, M. Ehara, K. Toyota, R. Fukuda, J. Hasegawa, M. Ishida, T. Nakajima, Y. Honda, O. Kitao, H. Nakai, T. Vreven, K. Throssell, J. A. Montgomery Jr, J. E. Peralta, F. Ogliaro, M. J. Bearpark, J. J. Heyd, E. N. Brothers, K. N. Kudin, V. N. Staroverov, T. A. Keith, R. Kobayashi, J. Normand, K. Raghavachari, A. P. Rendell, J. C. Burant, S. S. Iyengar, J. Tomasi, M. Cossi, J. M. Millam, M. Klene, C. Adamo, R. Cammi, J. W. Ochterski, R. L. Martin, K. Morokuma, O. Farkas, J. B. Foresman, D. J. Fox, *Gaussian 16 Rev. B.01*, Wallingford, CT, **2016**; d) H. Abul-Futouh, Y. Zagranyarski, C. Müller, M. Schulz, S. Kupfer, H. Görls, M. El-Khateeb, S. Gräfe, B. Dietzek, K. Peneva, W. Weigand, *Dalton Trans.* **2017**, *46*, 11180–11191; e) G. Knorr, D. Costabel, A. Skabeev, C. Neumann, J. Brossette, S. Kupfer, A. Turchanin, W. Weigand, K. Peneva, *Dyes Pigm.* **2022**, *198*, 109940; f) M. Staniszewska, S. Kupfer, J. Guthmuller, *J. Phys. Chem. C* **2019**, *123*, 16003–16013; g) M. Staniszewska, S. Kupfer, J. Guthmuller, *Chemistry* **2018**, *24*, 11166–11176; h) G. E. Shillito, S. Rau, S. Kupfer, *ChemCatChem* **2023**, *15*.

Manuscript received: September 22, 2023
Accepted manuscript online: December 22, 2023
Version of record online: January 12, 2024